CCS Chemistry

RESEARCH ARTICLE

Received: Jan. 5, 2022 | Accepted: Feb. 11, 2022 | Published: Mar. 18, 2022

Neither Fluorocarbons nor Silicones: Hydrocarbon-Based Water-Borne Healable Supramolecular Elastomer with Unprecedent Dual Resistance to Water and Organic Solvents

Shuitao Gao[1,2], Shasha Jiang[1,2], Jinwan Qi[1,2], Tongyue Wu[1,2], Wenkai Wang[1,2], Zhijie Liu[1,2], Bin Zhang[1,2*], Jianbin Huang[1,2] & Yun Yan[1,2*]

[1]*College of Chemistry and Molecular Engineering, Peking University, Beijing 100871,* [2]*Beijing National Laboratory for Molecular Sciences (BNLMS), Beijing 100190*

**Corresponding authors: yunyan@pku.edu.cn; binzhang@pku.edu.cn*

Cite this: *CCS Chem.* **2022**, 4, 3724–3734
DOI: 10.31635/ccschem.022.202201775

Except for fluorocarbons and silicones, few artificial materials display both water and organic solvent resistance. Herein, we report an artificial hydrocarbon-based supramolecular elastomer that displays unprecedented dual resistance to both water and organic solvents. This elastomer is formed in water with two water soluble components, folic acid (FA) and branched poly(ethylene imine) (b-PEI). The hydrogen bonding between the two components occurs immediately, which further promotes the hydrogen bonding between the FA, yielding folate quartets and their π–π stacking. These multiple noncovalent interactions work synergistically, leading to a hydrophobic, transparent, stretchable, healable, notch-insensitive, and recyclable elastomer that resists both water and organic solvents. The elastomer remains intact after storage in high humidity and organic solvents for months. Films generated by stretching the elastomer are very hydrophobic, and the contact angle of water on the elastomer is up to 112.3°. The damaged elastomers also exhibit water-assisted healable behavior. This work discloses a new paradigm of material synthesis that can inspire the fabrication of robust nonfluorocarbon and silicone-based materials with green strategies.

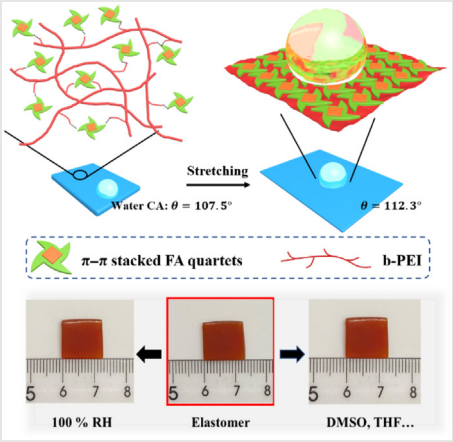

Self-assembly of folic acid and b-PEI leading to the formation of water-organic solvent dual-resistant elastomer

Keywords: folic acid, elastomer, quartets, π–π stacking, hydrogen bonding

DOI: 10.31635/ccschem.022.202201775
Citation: *CCS Chem.* **2022**, 4, 3724–3734
Link to VoR: https://doi.org/10.31635/ccschem.022.202201775

Introduction

Healable and recyclable organic materials that resist both water and organic solvents are very crucial for their applications.[1-4] This is especially true for elastomers, widely employed in electronic skin,[5-7] soft robots,[8-10] ionic conductors, and flexible sensors.[11-13] Endowing such dual resistance to them would reduce the risk of material damage caused by cleaning or accidental water or organic solvent exposure. Usually, hydrophobic elastomers can be damaged by organic solvents,[4,14] whereas hydrophilic ones are destroyed by water through a solubilization or swelling process.[15,16] Except for the environmentally unfriendly fluorocarbons and unstable silicones, few elastomers are able to resist both water and organic solvents.

Cleaning preparation has become urgent to achieve the global goal of carbon neutrality and peak carbon dioxide emission.[17] However, currently, most elastomers are prepared from organic solvents through multisteps.[18] Although some hydrogel elastomers are also fabricated, they usually shrink in the presence of organic solvents[19] and would swell upon contact with water.[1] Both changes would cause device breakage, which is unacceptable for an ideal elastomer required for practical applications. So far, it is still challenging to solve the dilemma of the cleaning preparation and the desired dual robustness toward both water and organic solvents.

To achieve this goal, herein we report that by combining the hydrophobic effect, π–π stacking, and hydrogen bonding between folic acid (FA) and branched poly(ethylene imine) (b-PEI) in water, the resultant materials are both resistant to high humidity and organic solvents (Scheme 1). The interaction between FA and b-PEI enhances the local concentration of FA, which facilitates the formation of folic quartets. These quartets then undergo π–π stacking, generating a hydrophobic hard core, which on the one hand serves as water insoluble supramolecular polymers that interact with b-PEI via hydrogen bonding. On the other hand, the multiple hydrogen bonding between FA and b-PEI renders sufficient organic solvent resistance. As such, this water-borne elastomer exhibits dual resistance to both water and organic solvents. Furthermore, this fresh elastomer displays instant self-healing ability, owing to the extensive and dynamic supramolecular interactions.[20] However, as the cut was aged in air for hours, the hydrophobic quartets migrated to the surface, which prohibits the hydrogen bonding between the carbonate groups and the amide groups. Fortunately, recycling of the elastomer is always possible by kneading the patches of the elastomers in the presence of a small amount of water, which makes the current elastomer an attractive material originated from cleaning preparation but with robust water and organic solvent resistance.

Experimental Section

Materials

FA hydrate (>98.0%) was purchased from Tokyo Chemical Industry Co., Ltd. Corporation (Shanghai, China) b-PEI (30 wt % in water, Mw = 100,000) was obtained

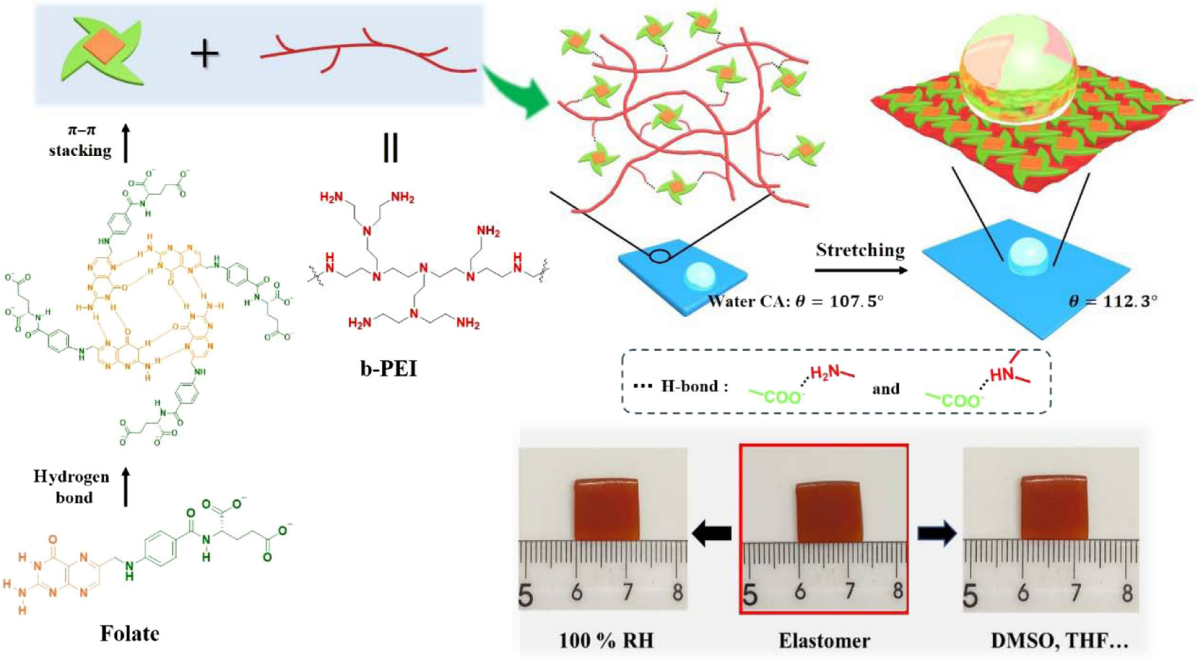

Scheme 1 | *Molecular structures of the ionized FA (folate) and b-PEI, and schematic illustration of the self-assembly of folate and b-PEI leading to the formation of elastomers resisting both humidity and organic solvents.*

DOI: 10.31635/ccschem.022.202201775
Citation: *CCS Chem.* **2022**, 4, 3724–3734
Link to VoR: https://doi.org/10.31635/ccschem.022.202201775

commercially from Beijing Hwrkchemical Co., Ltd (Beijing, China) and used without further purification. Gallium-indium eutectic was purchased from Sigma-Aldrich Corporation (Shanghai, China). Sodium hydroxide (NaOH) was purchased from Xilong Chemicals (Shantou, Guangdong, China) with purity above 99.0%. All the above chemicals were used as received. Water used in all experiments was purified by Milli-Q Advantage A10 ultrapure water system (Millipore S.A.S. 67120 Molsheim, France).

Preparation of the supramolecular elastomer

The aqueous solution of FA at a pH of 8.0 and the aqueous solution of branched PEI was mixed at the volume ratio of 1:1 under stirring. A yellow color water-immiscible coacervate was formed immediately. The sediment was collected and kneaded into a homogeneous ball, then compressed between two Teflon slides, followed by incubation under a relative humidity (RH) of 100% at room temperature for 2 days. The resultant elastomer sheet was transparent dark red and labeled as FA-bPEI-8-100 throughout the text. For mechanical strength measurements in organic solvents, the elastomer without incubation in 100% RH was used to demonstrate that the elastomer is not soluble in them, which was labeled as FA-bPEI-8. Immersion of FA-bPEI-8-100 in organic solvents will lead to FA-bPEI-8, due to the uptake of water by the organic solvents (except CH_2Cl_2).

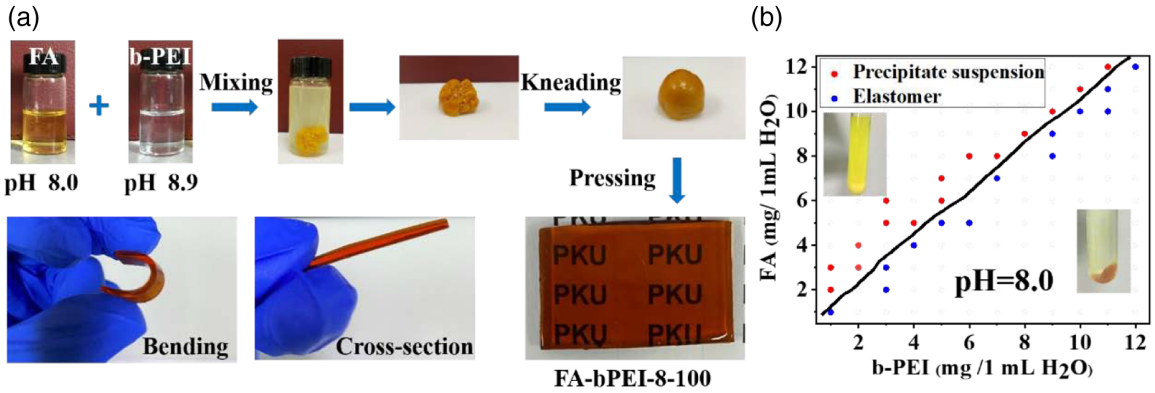

Figure 1 | *Preparation of the FA-bPEI-8-100 composite elastomer. (a) Photos of the samples at different stages and states. (b) Phase diagram of FA/b-PEI mixture at pH 8.0. The insets are the representative photos for the in situ precipitates and elastomers generated.*

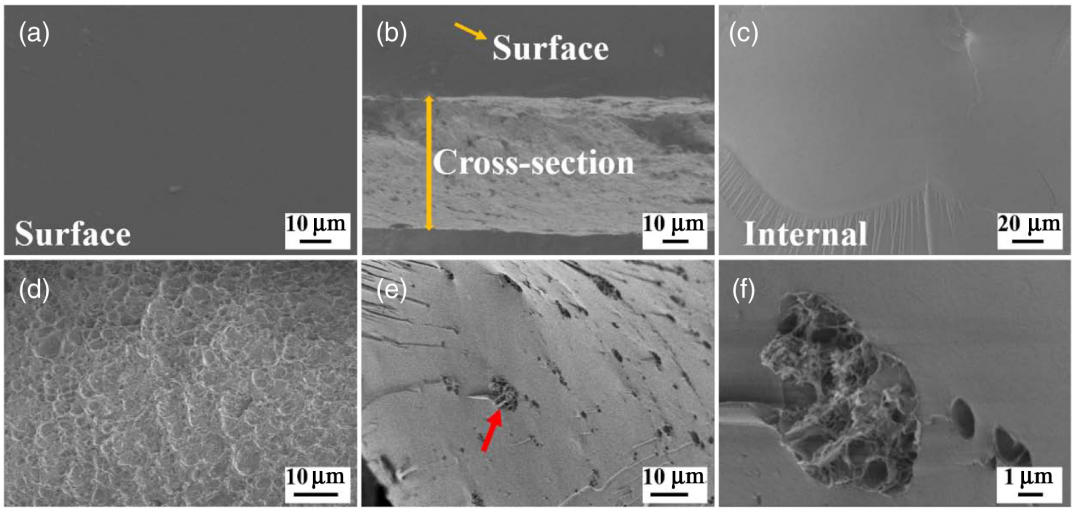

Figure 2 | *SEM image of the FA-bPEI-8-100 sheet under different conditions. (a) Surface, (b) cross-section, and (c) internal structure of the dry FA-bPEI-8-100 elastomer. (d) Surface, (e) cross section, and (f) the enlarged of the freeze-dried FA-bPEI-8-100 sheet.*

DOI: 10.31635/ccschem.022.202201775
Citation: *CCS Chem.* **2022**, 4, 3724–3734
Link to VoR: https://doi.org/10.31635/ccschem.022.202201775

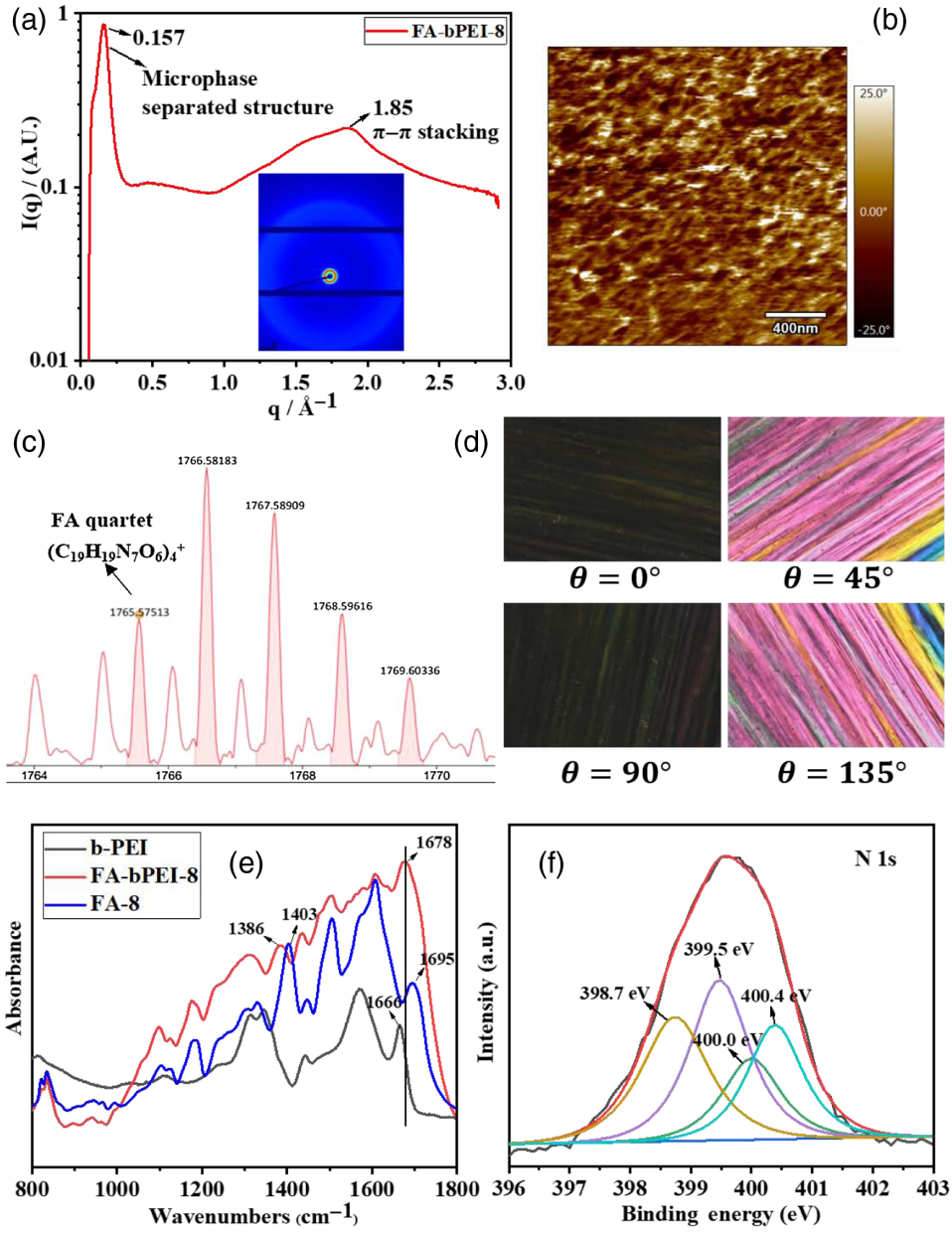

Figure 3 | *Characterization of the dried FA-bPEI-8 elastomer. (a) Wide-angle X-ray scattering (WAXS) profile of FA-bPEI-8. The inset shows the two-dimensional WAXS image. (b) AFM image of FA-bPEI-8. (c) High-resolution mass spectrometry of the FA-bPEI-8. (d) POM image of FA-bPEI-8 elastomer after stretching. (e) FT-IR spectroscopy of FA-8, b-PEI, and the FA-bPEI-8 sample. (f) XPS spectrum for N 1s of FA-bPEI-8 elastomer.*

Results and Discussion

Fabrication and characterization of the elastomer

The chemical structures of FA and b-PEI and the schematic illustration of the elastomer preparation are presented in Scheme 1 and Figure 1a. Because both compounds are pH-dependent, the variation of pH significantly impacts the interactions between FA and b-PEI. A coacervate was generated upon mixing the aqueous solution of FA and b-PEI in the wide pH range of 6.5~11.0 (Figure 1b and Supporting Information Figure S1). However, only the coacervate generated with the FA solution of pH 7.8~8.1 could be further transformed into free-standing healable elastomers after kneading (Figure 1a). Herein, the 0.012 g/mL FA solution at pH 8.0 was used. After the resultant coacervate was compressed between two Teflon slides and incubated in a RH of 100% at room temperature for 2 days, a flexible, dark red, transparent, and elastic rubber-like sheet of FA/b-PEI was obtained, which is termed FA-bPEI-8-100 in the following text.

DOI: 10.31635/ccschem.022.202201775
Citation: *CCS Chem.* **2022**, 4, 3724–3734
Link to VoR: https://doi.org/10.31635/ccschem.022.202201775

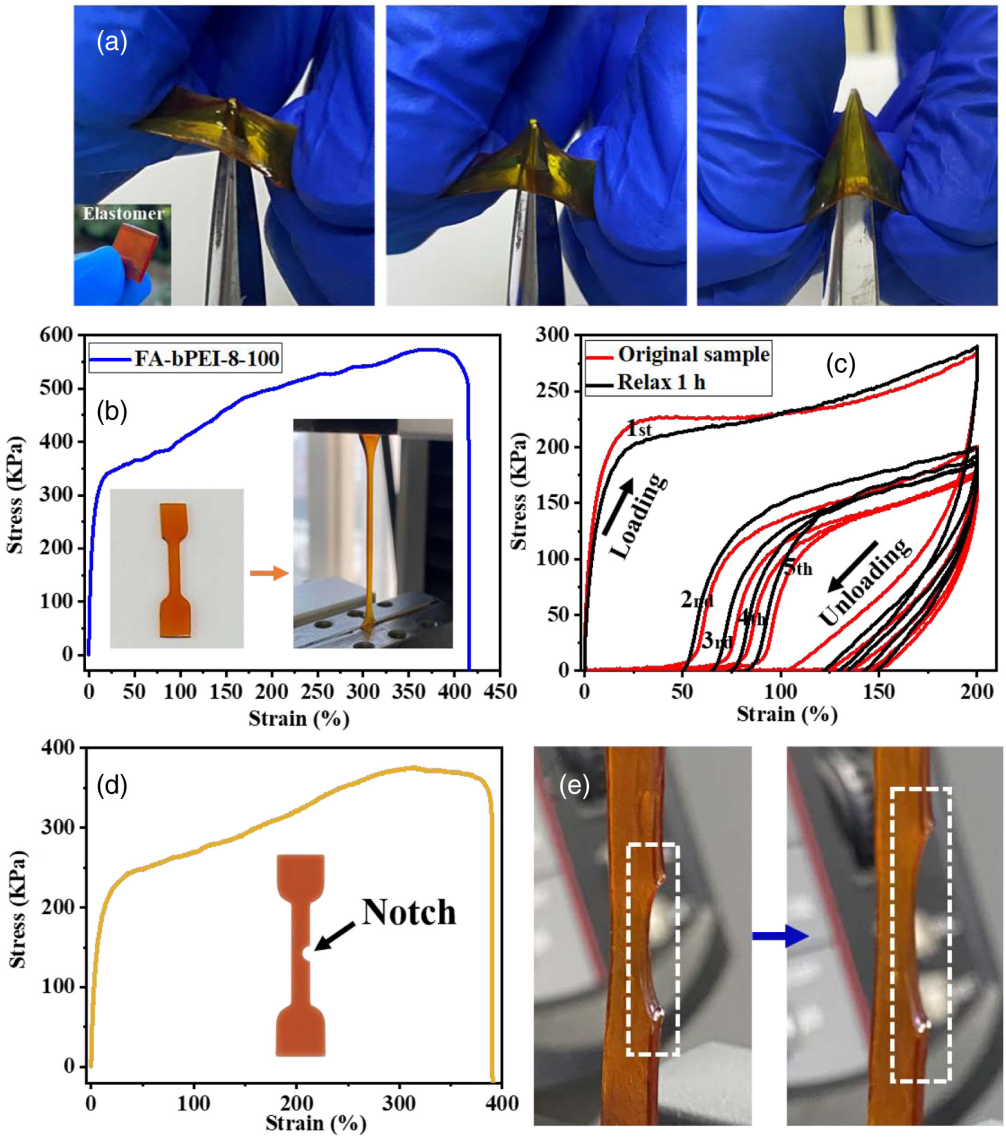

Figure 4 | *Mechanical property of the FA-bPEI-8-100 elastomer sheet. (a) The elastomer sheet cannot be punctured by sharp scissors. (b) Stress–strain curve of the FA-bPEI-8-100 elastomer sheet measured at RH = 100%. (c) Cyclic stress–strain curves of the elastomer sheet. (d) Tensile curve of the notched FA-bPEI-8-100 elastomer sheet. The inset is the demonstration of 1 mm notch in the 3.5 cm wide sheet. (e) The FA-bPEI-8-100 elastomer sheet can prevent crack propagation. The dashed line indicates the photo of the crack at different stretching state.*

The scanning electron microscopy (SEM) image in Figure 2a reveals that the surface of the elastomer sheet is very smooth, and its internal structure is very dense (Figures 2b and 2c). No pores are observed, indicating the content of water is not as high as it is in the folate hydrogels.[21,22] As the sample was freeze-dried, only a few pores were observed in the large area of the elastomer (Figures 2d–2f). Thermogravimetric analysis (TGA) measurement indicated that the water content in the FA-bPEI-8-100 elastomer was about 48% (Supporting Information Figure S2), which could be maximally enhanced to 57% after being fully immersed in water for 24 h (Supporting Information Figure S3). This means that the elastomer may have a water-shielding surface, which prevents free water penetration to its interior. Actually, the surface of the elastomer is very hydrophobic, which will be discussed later. The differential scanning calorimeter test showed the glass transition temperature (Tg) of the dry elastomer was approximately 116 °C (Supporting Information Figure S4). X-ray scattering measurements (Figure 3a and Supporting Information Figure S5) revealed a sharp peak at q = 0.157 A^{-1}, indicating the formation of hard phases with the average separation of 4.00 nm. Meanwhile, a broad peak occurred at q = 1.85 A^{-1}, corresponding to the characteristic π–π stacking distance of 0.34 nm. The microphase-separated

DOI: 10.31635/ccschem.022.202201775
Citation: *CCS Chem.* **2022**, 4, 3724–3734
Link to VoR: https://doi.org/10.31635/ccschem.022.202201775

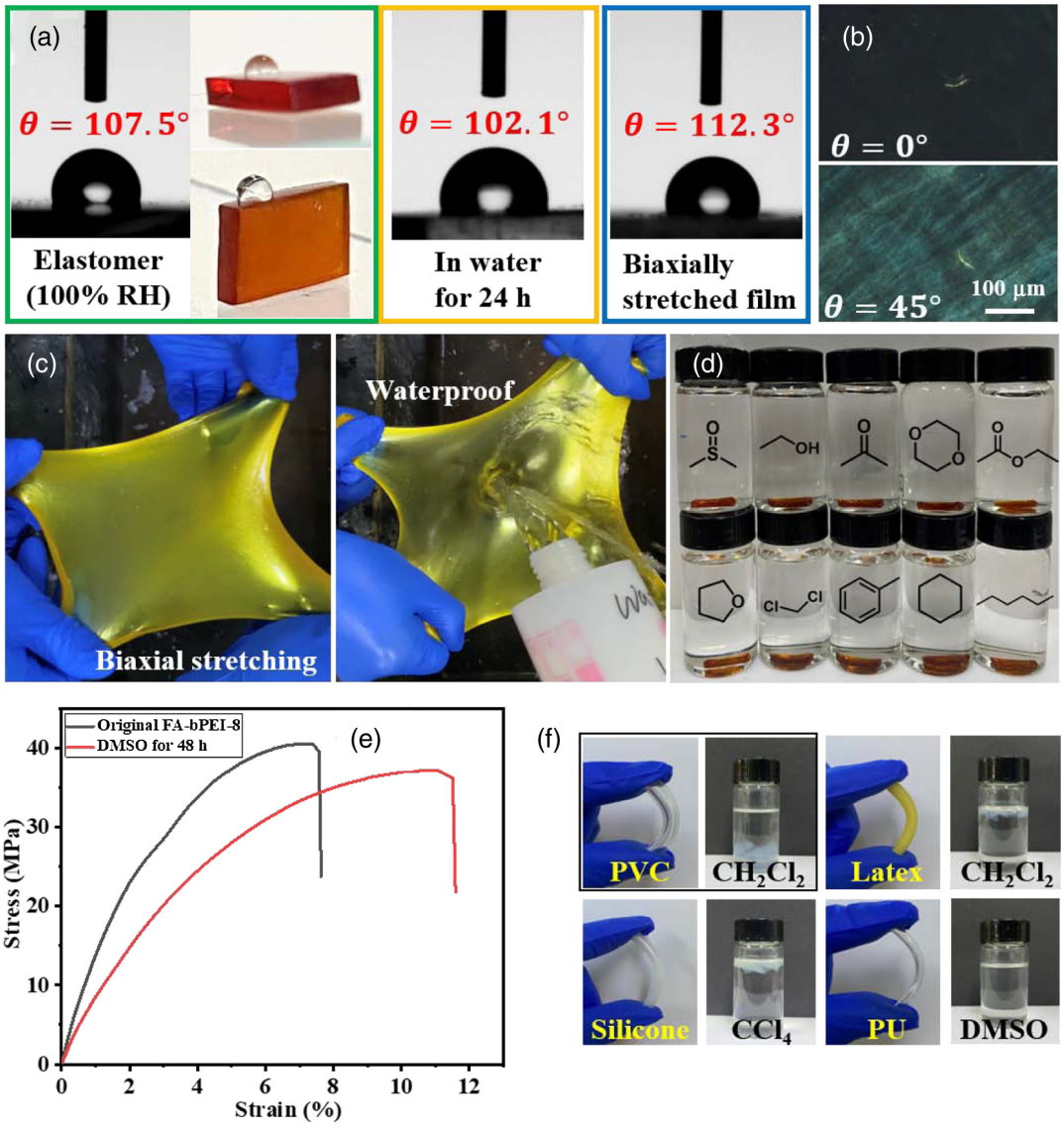

Figure 5 | *Water and organic solvent resistance of the FA-bPEI-8-100 elastomer sheet. (a) Images of the contact angles of water on the FA-bPEI-8-100 sheet at various states. (b) POM image of the biaxially stretched FA-bPEI-8-100 film. (c) Photo of the film upon biaxially stretching the FA-bPEI-8-100 sheet and its waterproof property demonstrated by pouring water. (d) Photographs of the FA-bPEI-8-100 sheet immersed in various organic solvents for 48 h. (e) Tensile stress–strain curves of the FA-bPEI-8 before and after being immersed into DMSO for 48 h. (f) The photos of the commercial elastomers dissolving or swelling in the organic solvents.*

structure was further verified by atomic force microscopy (AFM) (Figure 3b), which clearly shows both the soft segments (dark areas) and the hard segments (bright areas). The mass spectra manifested the predominant isotopic FA quartets in the range of m/z = 1765~1769 (Figure 3c),[23,24] indicating that the hard phases are composed of FA quartets via π–π stacking. In line with this, the sheet displayed significant birefringence under polarized optical microscopy (POM), which became more intensified after stretching (Figure 3d), owing to the stretching-induced alignment of the FA quartet stacks.[25–27] Fourier transform infrared (FT-IR) measurements (Figure 3e) suggest that hydrogen bonds have occurred between the COO^- group and the $-NH_2$ groups of b-PEI, as evidenced by the shifts of the N–H bending vibrations of primary amines of b-PEI from 1666 to 1678 cm^{-1} and the shift of the symmetric vibration of COO^- of FA from 1403 to 1386 cm^{-1}. The high-resolution N 1s X-ray photoelectron spectroscopy (XPS) in Figure 3f shows four binding energies at 399.5, 400.0, 400.4, and 398.7 eV, which are attributed to the N from the tertiary, secondary, and primary amine of b-PEI, and the C–N bond of the FA molecules. No protonated amine groups could be detected for the N1s electrons at the higher binding energy of 401.0~402.5 eV.[28–30]

DOI: 10.31635/ccschem.022.202201775
Citation: *CCS Chem.* **2022**, 4, 3724–3734
Link to VoR: https://doi.org/10.31635/ccschem.022.202201775

These results collectively indicate that it is the neutral amine groups that are primarily involved in the hydrogen bonding between b-PEI and stacked FA quartets (Scheme 1), leading to the self-coacervation of a supramolecular elastomer.

Mechanical properties

The resulting FA-bPEI-8-100 sheet exhibited excellent elasticity; it could not be easily damaged by the tip of sharp scissors (Figure 4a). The stress was up to 573 kPa at the strain of 416% in the environment of RH = 100% (Figure 4b). A big hysteresis loop was found in the first cycle of the cyclic loading-unloading stress–strain measurements at a strain of 200% (Figure 4c), indicating there is energy dissipation for the fracture of the dynamic interactions under strain. Consecutive cyclic loading–unloading tests revealed reduced hysteresis loops, manifesting that the recovery of the dynamic interactions in the stretched sheet takes time. However, after relaxing for 1 h, the elastomer demonstrated similar loading–unloading curves, indicative of the complete recovery of the elastomer to its initial state. Moreover, the elastic sheet was notch-insensitive. After a 1 mm notch was cut on the side of a stripe with a width of 3.5 mm, the sheet could still be stretched 390% rather than fracture along the crack spreading direction (Figures 4d and 4e). We noticed that on similar occasions, conventional elastomers, such as those formed with polydimethylsiloxane, polyurethane (PU), and styrene butadiene styrene block copolymer (saturated), could only sustain <150% strain.[31,32] The corresponding fracture energy (G_c) for the present FA-bPEI-8-100 sheet was calculated to be 5590.3 J m^{-2}, using the Greensmith equation of $G_C = \frac{6WC}{\sqrt{\lambda_c}}$. Here, C is the notch length, W is the integration of the stress–strain curve of the unnotched sample with the strain of λ_c.[33–35] During tensile stretching, the high density interchain H-bonds efficiently prevent the strain-induced crack propagation; meanwhile, the realignment of FA quartet stacks can dissipate the strain energy to prevent the rupture of main polymeric backbones. As a result, the dynamic rupture and reformation of the multiple noncovalent interactions reduces the stress density at the notch.[2,32,35]

Hydrophobicity and organic solvent resistance

Most water-borne composite materials are hydrophilic, and the solids of the composites usually can be hydrated to form hydrogel or coacervates that lose their structural strength and integrity at the high RH of 100% or in water.[15,36] However, the current FA-bPEI-8-100 sheet remained structurally intact and displayed unusual hydrophobicity. Figure 5a shows that the contact angle of water on the FA-bPEI-8-100 sheet was 107°, which only slightly decreased to 102° as the sheet was further immersed in water for 24 h. The Supporting Information Video S1 shows that as the sheet was placed in water, it remained floating on the surface of water. When being pressed into the bulk water, the adhered water rolled off the surface readily. This means that the surface of the sheet was rich in the hydrophobic FA quartets. Because hydrophobic materials have much smaller surface energy than hydrophilic ones, the location of FA quartets on the surface is advantageous to reduce the surface energy. We noticed that upon biaxially stretching, the contact angle of water on the material can be further enhanced to 112°. Meanwhile, considerable birefringence was observed under POM (Figure 5b). This was up to our expectation, since stretching would enhance the size of the self-assembled structures owing to a better alignment along the shear force.[25–27] Thus, the tightly packed FA quartets with their surface parallel to that of the film further improved the hydrophobicity (Scheme 1). A water-pouring experiment revealed that water will roll off of the stretched film just like it does on the surface of a lotus leaf (Figure 5c and Supporting Information Video S2). Line-drawing with a dyne pen (Supporting Information Figure S6) suggests that the surface tension for the FA-bPEI-8-100 sheet is about 38 mN/m, which is close to the surface tension of the aqueous solution of some cationic hydrocarbon surfactants.[37]

Strikingly, the elastomer sheet also displayed unusual organic solvent resistance, which was attributed to the extensive hydrogen bonding in the elastomer, as well as the excellent ability of FA to form stable quartets in organic solvent.[38–41] As the sheets were immersed in dimethyl sulfoxide (DMSO), ethanol, acetone, 1,4-dioxane, ethyl acetate, tetrahydrofuran (THF), methylene chloride, toluene, cyclohexane, and hexane, the sheet remained intact for 48 h (Figure 5d). Their weights were nearly unchanged (Table 1). The mechanical test

Table 1 | *The Weight Difference of the FA-bPEI-8 Elastomer Before and After Immersing in the Various Organic Solvents*

Organic Solvents	Original Weight (g)	The Weight after Immersing for 48 h (g)
DMSO	0.144	0.151
Ethanol	0.126	0.132
Acetone	0.164	0.164
1,4-Dioxane	0.138	0.139
Ethyl acetate	0.167	0.166
THF	0.163	0.165
Methylene chloride	0.142	0.143
Toluene	0.113	0.123
Cyclohexane	0.108	0.106
Hexane	0.154	0.156

DOI: 10.31635/ccschem.022.202201775
Citation: *CCS Chem.* **2022**, 4, 3724–3734
Link to VoR: https://doi.org/10.31635/ccschem.022.202201775

suggested that the mechanical properties were hardly affected (Figure 5e and Supporting Information Figure S7). In contrast, many other synthesized commercial elastomers, such as PU, polyvinyl chloride, latex, and silicone tube (Figure 5f), as well as composite materials based on polyelectrolyte and oppositely charged surfactants,[42] would be solubilized completely or suffer from excessive swelling at least in one of these organic solvents. So far, few composite materials and synthetic polymeric materials have been reported that exhibit sufficient stability both in water and in organic solvent. The FA-bPEI-8-100 sheet is nevertheless very prominent among the reported elastomers.

Healability

Integrating self-healing properties into high-performance elastomers is an effective way to prolong the material's longevity and durability.[9,43,44] It should be mentioned that although the elastomer is hydrophobic, healing of the

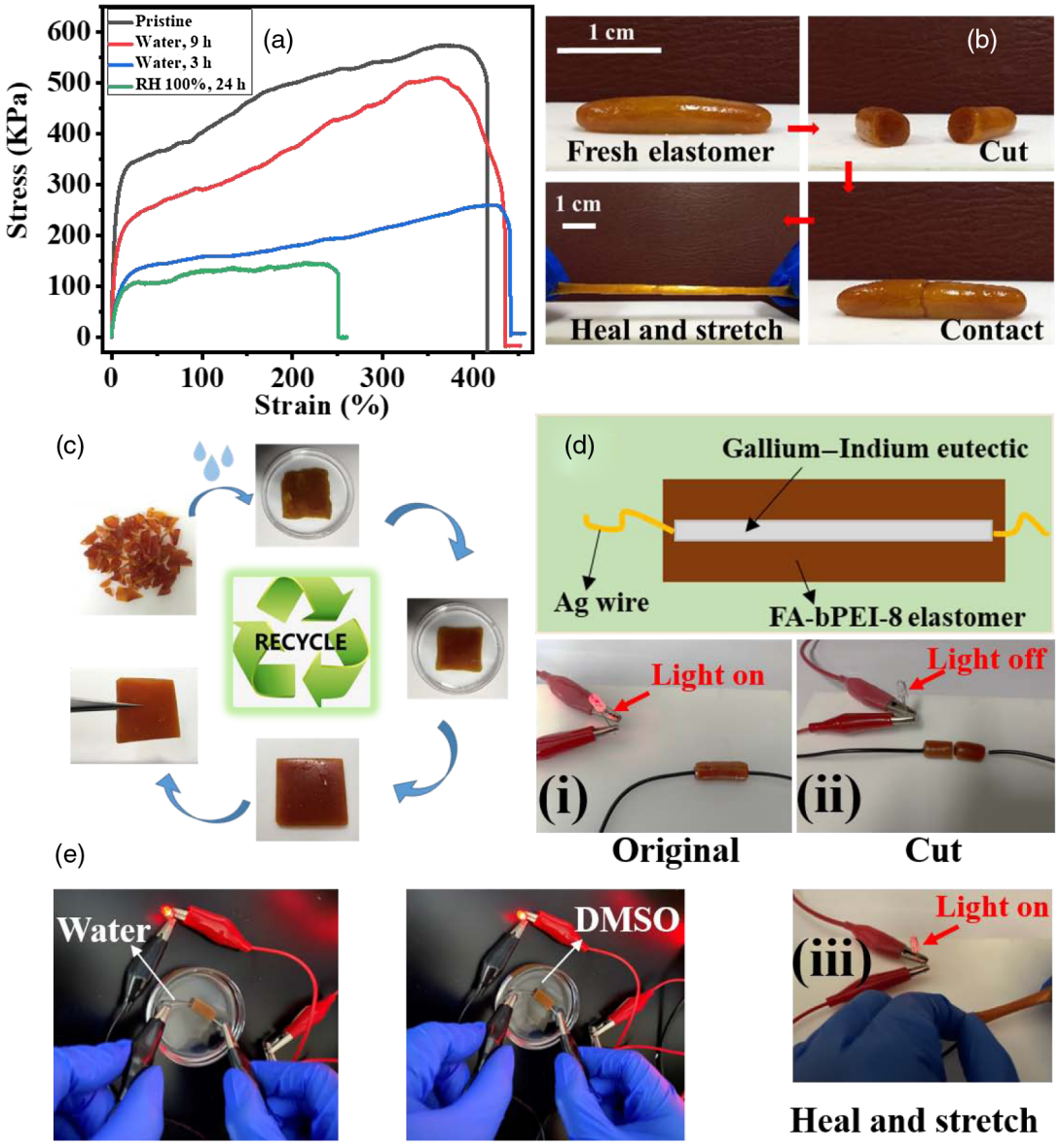

Figure 6 | *Self-healing and recycling ability of the FA-bPEI-8-100 elastomer. (a) Tensile stress–strain curves of the elastomer FA-bPEI-8-100 under different healing conditions. (b) Photos of the self-healing ability of the freshly prepared FA-bPEI-8 elastomer within 5 s. (c) Photos of the elastomer at different recycling stages facilitated by water activation. (d) Demonstration of the stretchable and self-healable electrical conductor of FA-bPEI-8-100/EGaIn made by injecting EGaIn into the freshly prepared FA-bPEI-8-100 elastomer. (i) The LED was lit when the FA-bPEI-8-100/EGaIn conductor at the original stage, and (ii) turned off after the conductor being cut. (iii) Healing of the conductor lights up the LED again. (e) The LED devices work properly as the conductor is immersed in water or DMSO.*

DOI: 10.31635/ccschem.022.202201775
Citation: *CCS Chem.* **2022**, 4, 3724–3734
Link to VoR: https://doi.org/10.31635/ccschem.022.202201775

material is still possible upon bringing the two water-activated parts together. Figure 5a shows that although the water-immersed elastomer still possesses a large contact angle of 102°, it has been decreased by 5° compared to the original 107°. Meanwhile, the stress decreased from 573 KPa to about 326 KPa, and the strain increased from 416% to 550% (Supporting Information Figure S8). This means that the material can be softened by water,[45] thus endowing sufficient mobility to the chains. After immersion in water for 9 h, followed by incubation in a RH = 100% humid environment for 20 h, the broken surface merged together. The toughness and the Young's modulus were recovered to 82.1% and 85.7%, respectively (Figure 6a). Strikingly, the freshly cut surface for the fresh elastomers can be healed within 5 s (Figure 6b), indicating the incomplete supramolecular interactions in the elastomer is beneficial to its self-healing ability. We inferred that immersion of the elastomer sheet in water would slowly solvate the hydrophilic domains, thus rendering sufficient mobility to the components to heal the damage.

Finally, as shown in Figure 6c, a recycled new elastomer can be obtained by pressing the water-activated sheet fragments at room temperature, due to the water-mediated reversible supramolecular interactions. The stress–strain curves in Supporting Information Figure S9 prove that the mechanical properties of the regenerated FA-bPEI-8-100 elastomer are almost the same as the original, demonstrating the high recycling ability of the current water-borne elastomer.

Taking advantage of its superior mechanical properties and self-healing ability, we fabricated a self-healing conductor with the freshly prepared FA-bPEI-8-100 elastomer by injecting liquid metal EGaIn into it.[12,31,46] FA-bPEI-8-100 on its own is not conductive and just acts as the encapsulation and supporting layer. As shown in Figure 6d, the light-emitting diode (LED) was lighted with this FA-bPEI-8-100/EGaIn conductor. However, the LED went out as the conductor was cut in half. When the two parts were reconnected, the conductivity recovered immediately, indicating sufficient healing of the conductor. Moreover, the healed conductor can be stretched again with the LED remaining on (Figure 6d). Because the material displays both water and organic solvent resistance, the LED device works properly when the elastomer is immersed in water and organic solvent (Figure 6e), demonstrating its ability to work in humid air and an environment full of organic vapor.

Conclusion

This work provides an unprecedented strategy for developing a robust hydrocarbon-based material that is resistant both to organic solvents and water with the commercial hydrocarbon-based compound of FA and b-PEI. The joint contribution of the hydrogen bonding between FA and b-PEI, the hydrogen bonding driven FA quartets and their π–π stacking are crucial for this excellent performance. Strikingly, the synergistic effect of these interactions also endows the supramolecular elastomer with excellent hydrophobic, notch-insensitive, self-healing and recyclable ability. This work shows that rationally designed water-based supramolecular interactions are very promising in creating nonfluorocarbon and nonsilicone-based robust materials, which is of great importance to the global goal of green chemistry and cleaning preparation.

Supporting Information

Supporting Information is available and includes Videos S1 and S2 and Figures S1–S9.

Conflict of Interest

The authors declare no conflicts of interest.

Funding information

This work was financially supported by the National Natural Science Foundation of China (grant nos. NSFC 22172004 and 21972003) and the Beijing National Laboratory for Molecular Sciences (BNLMS) for financial support.

References

1. Cao, Y.; Tan, Y. J.; Li, S.; Lee, W. W.; Guo, H.; Cai, Y.; Wang, C.; Tee, B. C. K. Self-Healing Electronic Skins for Aquatic Environments. *Nat. Electron.* **2019**, *2*, 75–82.
2. Kang, J.; Son, D.; Wang, G. N.; Liu, Y.; Lopez, J.; Kim, Y.; Oh, J. Y.; Katsumata, T.; Mun, J.; Lee, Y.; Jin, L.; Tok, J. B.; Bao, Z. Tough and Water-Insensitive Self-Healing Elastomer for Robust Electronic Skin. *Adv. Mater.* **2018**, *30*, e1706846.
3. Fujisawa, Y.; Asano, A.; Itoh, Y.; Aida, T. Mechanically Robust, Self-Healable Polymers Usable under High Humidity: Humidity-Tolerant Noncovalent Cross-Linking Strategy. *J. Am. Chem. Soc.* **2021**, *143*, 15279–15285.
4. Li, R. A.; Chen, G.; Fan, T.; Zhang, K.; He, M. Transparent Conductive Elastomers with Excellent Autonomous Self-Healing Capability in Harsh Organic Solvent Environments. *J. Mater. Chem. A* **2020**, *8*, 5056–5061.
5. Kim, S. M.; Jeon, H.; Shin, S. H.; Park, S. A.; Jegal, J.; Hwang, S. Y.; Oh, D. X.; Park, J. Superior Toughness and Fast Self-Healing at Room Temperature Engineered by Transparent Elastomers. *Adv. Mater.* **2018**, *30*, 1705145.
6. Li, F.; Xu, Z.; Hu, H.; Kong, Z.; Chen, C.; Tian, Y.; Zhang, W.; Bin Ying, W.; Zhang, R.; Zhu, J. A Polyurethane Integrating Self-Healing, Anti-Aging and Controlled Degradation for Durable and Eco-Friendly E-Skin. *Chem. Eng. J.* **2021**, *410*, 128363.

DOI: 10.31635/ccschem.022.202201775
Citation: *CCS Chem.* **2022**, 4, 3724–3734
Link to VoR: https://doi.org/10.31635/ccschem.022.202201775

7. Tan, Y. J.; Wu, J.; Li, H.; Tee, B. C. K. Self-Healing Electronic Materials for a Smart and Sustainable Future. *ACS Appl. Mater. Interfaces* **2018**, *10*, 15331–15345.
8. Cao, J.; Lu, C.; Zhuang, J.; Liu, M.; Zhang, X.; Yu, Y.; Tao, Q. Multiple Hydrogen Bonding Enables the Self-Healing of Sensors for Human-Machine Interactions. *Angew. Chem. Int. Ed.* **2017**, *56*, 8795–8800.
9. Tan, Y. J.; Susanto, G. J.; Anwar Ali, H. P.; Tee, B. C. K. Progress and Roadmap for Intelligent Self-Healing Materials in Autonomous Robotics. *Adv. Mater.* **2021**, *33*, e2002800.
10. Tan, M. W. M.; Thangavel, G.; Lee, P. S. Rugged Soft Robots Using Tough, Stretchable, and Self-Healable Adhesive Elastomers. *Adv. Funct. Mater.* **2021**, *31*, 2103097.
11. Ying, W. B.; Wang, G.; Kong, Z.; Yao, C. K.; Wang, Y.; Hu, H.; Li, F.; Chen, C.; Tian, Y.; Zhang, J.; Zhang, R.; Zhu, J. A Biologically Muscle-Inspired Polyurethane with Super-Tough, Thermal Reparable and Self-Healing Capabilities for Stretchable Electronics. *Adv. Funct. Mater.* **2021**, *31*, 2009869.
12. Zhang, L.; Liu, Z.; Wu, X.; Guan, Q.; Chen, S.; Sun, L.; Guo, Y.; Wang, S.; Song, J.; Jeffries, E. M.; He, C.; Qing, F. L.; Bao, X.; You, Z. A Highly Efficient Self-Healing Elastomer with Unprecedented Mechanical Properties. *Adv. Mater.* **2019**, *31*, e1901402.
13. Du, R.; Xu, Z.; Zhu, C.; Jiang, Y.; Yan, H.; Wu, H. C.; Vardoulis, O.; Cai, Y.; Zhu, X.; Bao, Z.; Zhang, Q.; Jia, X. A Highly Stretchable and Self-Healing Supramolecular Elastomer Based on Sliding Crosslinks and Hydrogen Bonds. *Adv. Funct. Mater.* **2019**, *30*, 1907139.
14. Lu, X.; Luo, Y.; Li, Y.; Bao, C.; Wang, X.; An, N.; Wang, G.; Sun, J. Polymeric Complex Nanoparticles Enable the Fabrication of Mechanically Superstrong and Recyclable Poly(aryl ether sulfone)-Based Polymer Composites. *CCS Chem.* **2020**, *2*, 524–532.
15. An, N.; Wang, X.; Li, Y.; Zhang, L.; Lu, Z.; Sun, J. Healable and Mechanically Super-Strong Polymeric Composites Derived from Hydrogen-Bonded Polymeric Complexes. *Adv. Mater.* **2019**, *31*, e1904882.
16. Guo, H.; Fang, X.; Zhang, L.; Sun, J. Facile Fabrication of Room-Temperature Self-Healing, Mechanically Robust, Highly Stretchable, and Tough Polymers Using Dual Dynamic Cross-Linked Polymer Complexes. *ACS Appl. Mater. Interfaces* **2019**, *11*, 33356–33363.
17. Chen, J. M. Carbon Neutrality: Toward a Sustainable Future. *Innovation (N Y)* **2021**, *2*, 100127.
18. Yang, X.; Liu, J.; Fan, D.; Cao, J.; Huang, X.; Zheng, Z.; Zhang, X. Scalable Manufacturing of Real-Time Self-Healing Strain Sensors Based on Brominated Natural Rubber. *Chem. Eng. J.* **2020**, *389*, 124448.
19. Çaykara, T.; Doğmuş, M. The Effect of Solvent Composition on Swelling and Shrinking Properties of Poly(acrylamide-co-itaconic Acid) Hydrogels. *Eur. Polym. J.* **2004**, *40*, 2605–2609.
20. Stefano, B.; Greenland, B. W.; Merino, D. H.; Weng, W.; Seppala, J.; Colquhoun, H. M.; Hayes, W.; Mackay, M. E.; Hamley, I. W.; Rowan, S. J. A Healable Supramolecular Polymer Blend Based on Aromatic π-π Stacking and Hydrogen-Bonding Interactions. *J. Am. Chem. Soc.* **2010**, *132*, 12051–12058.
21. Liu, K.; Zang, S.; Xue, R.; Yang, J.; Wang, L.; Huang, J.; Yan, Y. Coordination-Triggered Hierarchical Folate/Zinc Supramolecular Hydrogels Leading to Printable Biomaterials. *ACS Appl. Mater. Interfaces* **2018**, *10*, 4530–4539.
22. Liu, K.; Ma, C.; Wang, W.; Zang, S.; Cai, Y.; Chen, W.; Liu, Z.; Huang, J.; Yan, Y. A Metalloprotein-Inspired Thermo-Gene for Thermogels. *Inorg. Chem. Front.* **2020**, *7*, 4086–4091.
23. Gao, S.; Wang, W.; Wu, T.; Jiang, S.; Qi, J.; Zhu, Z.; Zhang, B.; Huang, J.; Yan, Y. Folic Acid-Based Coacervate Leading to a Double-Sided Tape for Adhesion of Diverse Wet and Dry Substrates. *ACS Appl. Mater. Interfaces* **2021**, *13*, 34843–34850.
24. Gao, S.; Qi, J.; Jiang, S.; Wu, T.; Wang, W.; Cai, Y.; Ma, C.; Zhang, B.; Huang, J.; Yan, Y. Green Wood Adhesives from One-Pot Coacervation of Folic Acid and Branched Poly(ethylene imine). *ACS Appl. Bio Mater.* **2021**, *4*, 7314–7321.
25. Li, L.; Li, W.; Geng, L.; Chen, B.; Mi, H.; Hong, K.; Peng, X.; Kuang, T. Formation of Stretched Fibrils and Nanohybrid Shish-Kebabs in Isotactic Polypropylene-Based Nanocomposites by Application of a Dynamic Oscillatory Shear. *Chem. Eng. J.* **2018**, *348*, 546–556.
26. Yuan, T.; Qu, X.; Cui, X.; Sun, J. Self-Healing and Recyclable Hydrogels Reinforced with in Situ-Formed Organic Nanofibrils Exhibit Simultaneously Enhanced Mechanical Strength and Stretchability. *ACS Appl. Mater. Interfaces* **2019**, *11*, 32346–32353.
27. Zhang, Q.; Chen, Y.; Wei, P.; Zhong, Y.; Chen, C.; Cai, J. Extremely Strong and Tough Chitosan Films Mediated by Unique Hydrated Chitosan Crystal Structures. *Mater. Today* **2021**, *51*, 27–38.
28. Yan, Y.-Z.; An, Q.-D.; Xiao, Z.-Y.; Zhai, S.-R.; Zhai, B.; Shi, Z. Interior Multi-Cavity/Surface Engineering of Alginate Hydrogels with Polyethylenimine for Highly Efficient Chromium Removal in Batch and Continuous Aqueous Systems. *J. Mater. Chem. A* **2017**, *5*, 17073–17087.
29. Razzaque, S.; Cheng, Y.; Hussain, I.; Tan, B. Synthesis of Surface Functionalized Hollow Microporous Organic Capsules for Doxorubicin Delivery to Cancer Cells. *Polym. Chem.* **2020**, *11*, 2110–2118.
30. Cui, Y.; Yin, L.; Sun, X.; Zhang, N.; Gao, N.; Zhu, G. A Universal and Reversible Wet Adhesive via Straightforward Aqueous Self-Assembly of Polyethylenimine and Polyoxometalate. *ACS Appl. Mater. Interfaces* **2021**, *13*, 47155–47162.
31. Ying, W. B.; Yu, Z.; Kim, D. H.; Lee, K. J.; Hu, H.; Liu, Y.; Kong, Z.; Wang, K.; Shang, J.; Zhang, R.; Zhu, J.; Li, R. W. Waterproof, Highly Tough, and Fast Self-Healing Polyurethane for Durable Electronic Skin. *ACS Appl. Mater. Interfaces* **2020**, *12*, 11072–11083.
32. Guo, H.; Han, Y.; Zhao, W.; Yang, J.; Zhang, L. Universally Autonomous Self-Healing Elastomer with High Stretchability. *Nat. Commun.* **2020**, *11*, 2037.
33. Greensmith, H. W. Rupture of Rubber. X. The Change in Stored Energy on Making a Small Cut in a Test Piece Held in Simple Extension. *J. Appl. Polym. Sci.* **1963**, *7*, 993–1002.

DOI: 10.31635/ccschem.022.202201775
Citation: *CCS Chem.* **2022**, 4, 3724–3734
Link to VoR: https://doi.org/10.31635/ccschem.022.202201775

34. Wu, J.; Cai, L. H.; Weitz, D. A. Tough Self-Healing Elastomers by Molecular Enforced Integration of Covalent and Reversible Networks. *Adv. Mater.* **2017**, *29*, 1702616.
35. Li, Z.; Zhu, Y. L.; Niu, W.; Yang, X.; Jiang, Z.; Lu, Z. Y.; Liu, X.; Sun, J. Healable and Recyclable Elastomers with Record-High Mechanical Robustness, Unprecedented Crack Tolerance, and Superhigh Elastic Restorability. *Adv. Mater.* **2021**, *33*, e2101498.
36. Voorhaar, L.; Hoogenboom, R. Supramolecular Polymer Networks: Hydrogels and Bulk Materials. *Chem. Soc. Rev.* **2016**, *45*, 4013–4031.
37. Yan, Y.; Huang, J.; Li, Z.; Zhao, X.; Zhu, B.; Ma, J. Surface Properties of Cationic Bolaamphiphiles and Their Mixed Systems with Oppositely Charged Conventional Surfactant. *Colloids Surf. A* **2003**, *215*, 263–275.
38. Davis, J. T.; Spada, G. P. Supramolecular Architectures Generated by Self-Assembly of Guanosine Derivatives. *Chem. Soc. Rev.* **2007**, *36*, 296–313.
39. Stefan, L.; Monchaud, D. Applications of Guanine Quartets in Nanotechnology and Chemical Biology. *Nat. Rev. Chem.* **2019**, *3*, 650–668.
40. Dash, J.; Saha, P. Functional Architectures Derived from Guanine Quartets. *Org. Biomol. Chem.* **2016**, *14*, 2157–2163.
41. Arnal-Hérault, C.; Pasc, A.; Michau, M.; Cot, D.; Petit, E.; Barboiu, M. Functional G-Quartet Macroscopic Membrane Films. *Angew. Chem. Int. Ed.* **2007**, *119*, 8561–8565.
42. Jin, H.; Xie, M.; Wang, W.; Jiang, L.; Chang, W.; Sun, Y.; Xu, L.; Zang, S.; Huang, J.; Yan, Y.; Jiang, L. Pressing-Induced Caking: A General Strategy to Scale-Span Molecular Self-Assembly. *CCS Chem.* **2020**, *2*, 98–106.
43. Utrera-Barrios, S.; Verdejo, R.; López-Manchado, M. A.; Hernández Santana, M. Evolution of Self-Healing Elastomers, from Extrinsic to Combined Intrinsic Mechanisms: A Review. *Mater. Horizons* **2020**, *7*, 2882–2902.
44. Islam, S.; Bhat, G. Progress and Challenges in Self-Healing Composite Materials. *Mater. Adv.* **2021**, *2*, 1896–1926.
45. Zhang, Q.; Deng, Y. X.; Luo, H. X.; Shi, C. Y.; Geise, G. M.; Feringa, B. L.; Tian, H.; Qu, D. H. Assembling a Natural Small Molecule into a Supramolecular Network with High Structural Order and Dynamic Functions. *J. Am. Chem. Soc.* **2019**, *141*, 12804–12814.
46. Chen, G.; Deng, X.; Zhu, L.; Handschuh-Wang, S.; Gan, T.; Wang, B.; Wu, Q.; Fang, H.; Ren, N.; Zhou, X. Recyclable, Weldable, Mechanically Durable, and Programmable Liquid Metal-Elastomer Composites. *J. Mater. Chem. A* **2021**, *9*, 10953–10965.

DOI: 10.31635/ccschem.022.202201775
Citation: *CCS Chem.* **2022**, 4, 3724–3734
Link to VoR: https://doi.org/10.31635/ccschem.022.202201775